ELSEVIER

Colloids and Surfaces
A: Physicochemical and Engineering Aspects 128 (1997) 225–242

COLLOIDS AND SURFACES A

Effects of lung surfactant specific protein SP-B and model SP-B peptide on lipid monolayers at the air–water interface

Ka Yee C. Lee [a], Michael M. Lipp [a], Joseph A. Zasadzinski [a,*], Alan J. Waring [b]

[a] *Department of Chemical Engineering, University of California, Santa Barbara, CA 93106, USA*
[b] *Department of Pediatrics, Drew University – King Medical Center, and University of California, Los Angeles, CA 90024, USA*

Received 14 August 1997

Abstract

Lung surfactant, a mixture of dipalmitoylphosphatidylcholine, phosphatidylglycerols, fatty acids and four lung surfactant specific proteins, forms tightly packed monolayers at the alveolar interface which are capable of lowering the normal air–water surface tension to almost zero. Isolating the roles of the individual components of lung surfactant is essential to understanding the biophysics of surfactant functioning and to developing new low-cost replacement surfactants. We have used fluorescence microscopy to show that both the full length lung surfactant specific protein SP-B_{1-78} and a shorter model peptide SP-B_{1-25} alter the phase behavior and surface morphology of palmitic acid (PA) monolayers. PA is an important component of both natural and replacement lung surfactants. Both the protein and the peptide inhibit the formation of condensed phase in monolayers of PA, resulting in a new fluid PA–protein phase. This fluid phase forms a network that separates condensed phase domains at coexistence. The network persists to high surface pressures, altering the nucleation, growth and morphology of monolayer collapse structures, leading to lower surface tensions on compression and more reversible respreading on expansion, factors essential to the in vivo performance of both natural and replacement lung surfactants. The network is stabilized by the low line tension between the fluid phase and the condensed phase as confirmed by the formation of extended linear domains or "stripe" phases. Similar stripes are found in monolayers of fluorescein-labeled SP-B_{1-25}, suggesting that the reduction in line tension is due to the protein. The peptide retains many of the essential functions of the full length protein and may be a lower cost substitute in replacement surfactants. © 1997 Elsevier Science B.V.

Keywords: Collapse; Homogeneous nucleation; Lipid–protein interactions; Lung surfactant; Monolayer

1. Introduction

The lungs provide an interface for the exchange of oxygen and carbon dioxide between the blood stream and the atmosphere. In order to facilitate exchange, a large interfacial area is required, about 1 m^2 per kilogram of body mass. The expansion and contraction of such a large area involves a significant expenditure of work against surface tension forces. To reduce the work of breathing, a mixture of lipids and proteins, commonly known as lung surfactant, produced by type II alveolar pneumocytes, lines the airspaces of the lungs of all mammalian species. This mixture stabilizes the lung alveoli during breathing by varying the air–surfactant interfacial tension according to alveolar curvature, ensuring that alveoli neither collapse

* Corresponding author. Fax: +1 805 893 4731;
e-mail: gorilla@engineering.ucsb.edu

PII S0927-7757(96)03919-2

nor rupture, while minimizing the work of breathing. The interfacial tension is changed by rapid adsorption, desorption, and compression of surfactant at the interface during each breathing cycle [1–3].

Deficiency or inactivation of lung surfactant are contributory factors to a number of pulmonary diseases. A deficiency of surfactant at birth, often due to premature delivery, is responsible for the development of neonatal respiratory distress syndrome (RDS) [4,5]. Inactivation of lung surfactant, perhaps as a result of pulmonary edema, is probably involved in the development of adult RDS [6–9]. Because of the serious morbidity and high mortality of these syndromes, research on surfactant replacement therapy has received significant attention in recent years [10]. Administration of exogenous natural surfactants has been proven to be an effective form of treatment for neonatal RDS [11], but only limited supplies of human lung surfactant are available, and the use of animal sources introduces potential problems with immunological responses, purity and reproducibility. The costs associated with the recruitment and purification of either human or animal surfactants are significant, especially for the lung surfactant specific protein SP-B that appears to be necessary to surfactant function in vivo [12–14]. As a result there have been several efforts to replace SP-B by peptides based on the full length protein [15–18], simple model peptides that mimic the basic structure of SP-B [19], or even simple polycations [17,20]. Developing a purely synthetic surfactant, however, requires a thorough understanding of the roles of the individual lipid and protein constituents of natural lung surfactant to identify the essential biophysical or biochemical function of each component.

Lung surfactant consists primarily of saturated dipalmitoylphosphatidylcholine (DPPC), unsaturated phosphatidylcholine (PC) and phosphatidylglycerol (PG), palmitic acid (PA), and lung surfactant specific proteins. Four such proteins have been identified, and are termed SP-A, -B, -C, and -D. SP-A and SP-D are large proteins that appear to convey long-range order on lipids and are believed to be necessary for surfactant transport and secretion, while SP-B and SP-C are small hydrophobic proteins that enhance the adsorption and activity of the surfactant lipids at the air–water interface [2,21,22].

DPPC, the major component of human lung surfactant, is capable of reducing the normal air–water surface tension (72 mN m^{-1}) to almost zero by forming monolayers that do not collapse at surface pressures below 70 mN m^{-1} [23]. However, DPPC by itself is a poor replacement surfactant because it forms rigid, multilamellar structures in solution that do not effectively form monolayers under physiological conditions [24,25]. The apparent role of the anionic PG and PA in natural and many replacement lung surfactants is to fluidize and separate the normally rigid DPPC bilayers in solution to enhance dispersion of the surfactant and increase absorption to interfaces [24,25]. PA, for instance, is an important additive to many exogenous surfactants [26]. It is believed to enhance surface activity and partially counteract inhibition by blood proteins [25,27–29]. However, PA does not prevent inhibition by blood proteins in synthetic mixtures that do not contain SP-B [30].

A minimum surface tension of less than 10 mN m^{-1} (corresponding to a minimum collapse pressure of more than 60 mN m^{-1}; see Fig. 1) is one of the essential features of natural lung surfactants or viable synthetic mixtures [4]. However, the monolayer collapse pressures of anionic lipids and fatty acids are typically much less than that of DPPC; PA films, for instance, collapse at around 40 mN m^{-1}. The lower collapse pressures result in the ejection of these components when anionic lipid–DPPC mixed monolayers are under sufficient compression. This effect has led to the belief that anionic lipids and fatty acids are "squeezed out" of lung surfactant monolayers during the exhalation portion of the breathing cycle [25,27–29]. We show that one role of SP-B is to alter the isotherms of fatty acid monolayers so that they resemble those of DPPC. In particular, the collapse pressure of the fatty acid monolayer is increased to nearly 70 mN m^{-1} and a highly compressible region of the isotherm is created at large areas per molecule. These changes in the fatty acid isotherm eliminate the driving force for "squeeze-out" of the fatty acid from the mixed

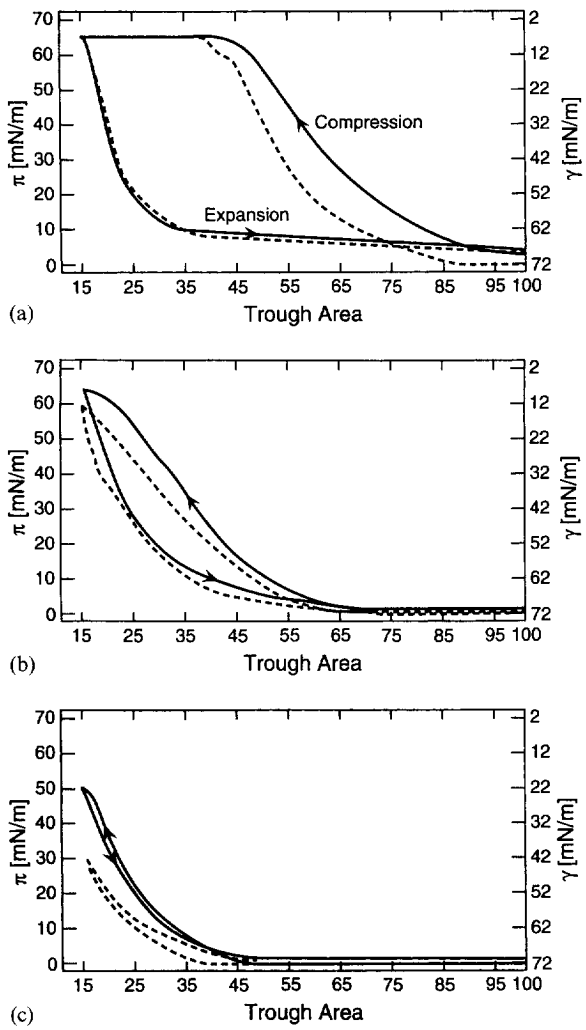

Fig. 1. Wilhelmy balance compression and expansion tracings of pressure–area curves for model lung surfactant dispersions containing: (A) DPPC:PG:PA:SP-B_{1-25}, 68:21:9:3 w/w; (B) DPPC:PG:PA:SP-B_{1-25}, 68:21:6:3 w/w; and (C) DPPC:PG:PA, 68:21:9 w/w. Displayed are the first (- - -) and fifth (———) compression cycles of dispersions on 154 mM saline solution. The abscissa is displayed in percentage of trough area available to the surfactant monolayer. 25 μg of dispersion in 10 μl of saline was applied to the surface of a Kim Ray Langmuir–Whilhelmy surface balance of 51.5 cm^2 surface area at 25°C. The compression–expansion cycle took 90 s to complete. The DPPC:PG:PA:SP-B_{1-25} 68:21:9:3 w/w dispersion raises the surface pressure immediately as the surface area is reduced, and the hysteresis between expansion and compression cycles obtained on the first compression is repeated on the fifth and subsequent compressions. The other tracings demonstrate diminished surface activity, especially a diminished hysteresis between compression and expansion cycles and a lower maximum surface pressure (higher minimum surface tension).

surfactant monolayer and lead to lower surface tensions of the mixed lung surfactant. This suggests a synergistic effect between PA and SP-B that results in both lipid and protein being retained in the primarily DPPC surfactant monolayer on compression [17].

However, isotherm studies alone cannot provide the molecular mechanisms by which SP-B alters monolayer properties. In this paper, we present both isotherm and fluorescence microscopy results on mixed PA and SP-B monolayers, and show how the addition of the peptide alters the surface morphology of fatty acid monolayers leading to higher collapse pressures. We also compare the morphological effects produced by the shorter model peptide SP-B_{1-25} with those caused by the full length SP-B_{1-78} protein. Our fluorescence images show that both the full length SP-B_{1-78} protein and the peptide SP-B_{1-25} [15,16] insert into PA monolayers and form a new "fluid" phase that inhibits the formation of condensed phases at all surface pressures. This protein-induced fluid phase forms a network that breaks up the remaining condensed phase domains at all surface pressures up to collapse. By shrinking the size of the condensed phase domains, the network of protein-rich fluid phase reduces the likelihood of heterogeneous nucleation of monolayer collapse, leading to lower ultimate surface tensions on compression, together with smaller and more homogeneous collapse structures that are easier to respread on expansion. These monolayer properties are directly related to important physiological consequences such as decreased work of breathing and increased alveolar stability [4]. The fluid phase network is stabilized by the low line tension between the fluid phase and the condensed phase domains. This low line tension is confirmed by our observations of extended linear domains or "stripe" phases at low surface pressures [31,32]. Similar stripe phases are found in monolayers of fluorescein-labeled SP-B_{1-25}, suggesting that SP-B lowers the two-dimensional line tension between phases, in addition to increasing the ratio of fluid to condensed phases. The close correspondence between the morphology and phase behavior induced by SP-B_{1-25} and the full length protein suggest that

the peptide might be a lower cost substitute in a purely synthetic replacement surfactant.

2. Experimental

2.1. Materials

SP-B is a lung surfactant-specific, 8.6 kD reduced molecular weight, amphiphilic protein which possesses eight net positive charges. The full length human 78-amino acid sequence (see Fig. 2(A)) of surfactant protein SP-B_{1-78} was synthesized on a 0.25 mmol scale with a 431A peptide synthesizer from Applied Biosystems (Foster City, CA, USA) using FastMoc™ chemistry [33]. A Wang Fmoc-L-Serine(OtBu) resin purchased from Applied Biosystems was used for synthesis. Amino acid residues 26–59 were double coupled, while all other residues were single coupled. After cleavage from the resin, the peptide was purified by reverse phase high performance liquid chromatography (HPLC) with a C4 column from Vydac (Hesperia, CA, USA) using a water–acetonitrile gradient containing 0.1% trifluoroacetic acid. The expected relative molecular mass was confirmed by electrospray mass spectrometry. The formation of disulfide bonds was facilitated using EKATHIOX™ resin from Ekagen Corp. (Palo Alto, CA, USA). Oxidation with EKATHIOX™ resin was carried out by the addition of a 1 mM peptide solution of TFE/water (9:1 v/v) to a 10-fold molar excess of the resin active group to peptide thiol. The reaction was allowed to proceed for 6 h before the peptide in solution was separated from the resin by centrifugation (1000*g* for 10 min). The monomeric oxidized state was confirmed by matrix-assisted laser desorption-time of flight (MALDI-TOF) mass spectroscopy.

A

```
     1          +   ++      +25
NH2-FPIPLPYCWLCRALIKRIQAMIPKG
        +          +          50
ALRVAVAQVCRVVPLVAGGICQCLA
  +        -    +          +   +  78
ERYSVILLDTLLGRMLPQLVCRLVLRCS-COOH
```

B

```
     1          +   ++      +25
NH2-FPIPLPYCWLCRALIKRIQAMIPKG-COOH
```

Fig. 2. Amino acid sequence for (A) the full length SP-B_{1-78} human lung surfactant protein, and (B) the N-terminal shorter model peptide SP-B_{1-25}. In each sequence, the charged residues are indicated with a plus or a minus sign.

The 25-residue shorter model peptide representing the N-terminal amino acid sequence, SP-B_{1-25}, has a reduced relative molecular mass of 2.9 kD and four positive charges. The sequence of this shorter model peptide is shown in Fig. 2(B). Synthesis was carried out by the solid-phase method using an Fmoc strategy with an Applied Biosystems 431A peptide synthesizer. The crude peptides were purified by a Vydac C4-column reversed-phase HPLC with a mixture of water, acetonitrile, and 0.1% trifluoroacetic acid. Solvents from HPLC and ion-pairing agents were removed from the purified peptides by vacuum centrifugation, and the expected molecular mass of the peptide was obtained by fast atom bombardment mass spectrometry or electrospray mass spectroscopy (UCLA Center for Molecular and Medical Sciences Mass Spectrometry). Quantitative amino acid composition for the peptide was determined at the UCLA Protein Microsequencing Facility.

The fluorescein derivative of SP-B_{1-25} with linkages at cysteine residues 8 and 11 was synthesized by slowly adding a five-fold excess of fluorescein-5-maleamide from Molecular Probes (Eugene, OR, USA) in dimethylformamide to the peptide in 10 mM phosphate buffer (pH 6.5). The mixture was bath sonicated for 5 min and vortexed immediately for 1 h at 25°C. The reaction was then quenched with a two-fold excess of cysteine and the reaction mixture dialyzed against distilled water overnight. The peptide was then freeze-dried and purified by reverse phase HPLC.

Palmitic acid (99% pure) was purchased from Sigma Chemical Co. (St. Louis, MO, USA) and was used without further purification. *N*-7-Nitrobenz-2-oxa-1,3-diazol-4-yl-hexadecylamine (NBD-HDA) was purchased from Molecular Probes (Eugene, OR, USA). Protein stock solutions were made using a 4:1 chloroform/methanol mixture, while PA stock solutions were made with chloroform. Spreading solutions of various con-

centrations of PA and protein were made from stock solutions with chloroform (Fisher spectranalyzed) as the solvent. All subphases were prepared using 18 MΩ water obtained from a Milli-Q UV Plus system (Millipore, Bedford, MA, USA). To mimic physiological conditions, $NaHCO_3$-buffered (pH 6.9) 0.15 M NaCl solution was used as the subphase for some experiments.

2.2. Langmuir trough

Cyclic measurements that traced the surface pressure of lung surfactant upon successive compressions and expansions were made using a Kim Ray Langmuir–Wilhelmy surface balance of 51.5 cm^2 surface area. All other experiments were carried out in a customized Langmuir trough which allowed simultaneous monitoring of surface morphology and phase behavior of the monolayer. Various PA/SP-B_{1-78} and PA/SP-B_{1-25} mixtures were spread quantitatively onto either a pure water or a buffered saline subphase at temperatures both above and below the triple point of PA [34]. Monolayers were formed at a highly expanded state; the monolayer area was compressed at various speeds ranging from 0.01 to 0.05 $Å^2$ per molecule per second. For quantitative comparisons, the compression speed was held constant within each set of measurements.

2.3. Surface pressure measurements

The surface pressure π is the difference in surface tension between the bare water surface tension (72 mN m^{-1}) and that when a monolayer is absorbed. A Wilhelmy plate system (K&R, Mainz, Germany) was used to detect changes in surface pressure as the monolayer was being compressed.

2.4. Fluorescence microscopy

Fluorescence microscopy makes possible the direct visualization of the surface morphology of monolayers at the air–water interface. The contrast is obtained by incorporating a small amount of fluorescent dye into the spreading solution. The fluorescent dye molecules preferentially partition into the less ordered phase, because the more condensed or better ordered phase has tighter packing and excludes the dye. This results in a brighter liquid-expanded phase and a darker liquid-condensed phase. In our case, the dye NBD-HDA used in all the experiments quenches when it is in contact with the subphase, rendering the gaseous phase black. A modified Nikon Optiphot microscope with a 40× long working distance objective was coupled to a Silicon Intensified Target camera for imaging. Details of the experimental setup has been presented elsewhere [35].

3. Results and discussions

Experimental investigations and surfactant replacement therapies utilizing SP-B are expensive because of the difficulty of obtaining SP-B from animal or human sources. Therefore, we have focused on the study of amphipathic peptides of the amino-terminal residues (1–25) of SP-B, known as SP-B_{1-25} (Fig. 2(B)), which contains four positively charged residues [15,16]. Other researchers have investigated other sequences of SP-B, or even simpler amino acid sequences that mimic certain aspects of SP-B [19,24,36,37]. The surface behavior of model lung surfactant mixtures (containing DPPC:PG in a ratio of 68:21 w/w) indicates that low surface tension monolayers, similar to those of natural lung surfactant, are obtained with 9% w/w PA and 3% w/w SP-B_{1-25} (Fig. 1(A)) and improve oxygenation in animal models [15,16]. A lower percentage of PA and deficiency of SP-B_{1-25} resulted in diminished surface activity of the surfactant (Fig. 1(B,C)). This is not surprising because PA is a significant fraction of natural lung surfactant, and is commonly added to both naturally derived and synthetic replacement lung surfactants to enhance performance [26]. As a result of these studies, we have focused on examining binary mixtures of PA and SP-B_{1-78} or the peptide SP-B_{1-25} to determine the origin of these effects.

3.1. Pure water subphase at 16°C

Below the triple point of pure PA monolayers which occurs at about 25°C, the gaseous phase

turns into the liquid-condensed phase without going through the liquid-expanded phase. The isotherm of the fatty acid alone showed two distinct condensed phases: a compressible liquid-condensed phase (Fig. 3(A), a to b), and a second incompressible, solid-condensed phase (b to c), followed by collapse at about 43 mN m^{-1}. This temperature was chosen so that any fluidization effect due to the presence of protein resulting in a liquid-expanded phase would be unambiguous. With the addition of both the full length SP-B_{1-78} and the shorter model peptide SP-B_{1-25}, two effects were observed. Firstly, the monolayer collapse pressure was significantly increased (see Fig. 3(A)), suggesting that the presence of the protein stabilized the PA film and helped it withstand higher compression. Secondly, phase transitions occurred at a higher area per fatty acid molecule, indicating that the water-soluble peptide was retained in the monolayer. When the fraction of peptide was increased, the onset of the first pressure rise (see lift-off points in Fig. 3(A)) occurred at successively larger surface areas. The only difference between the two peptides appears to be that the full length SP-B_{1-78} is better retained in the monolayer than the shorter model peptide SP-B_{1-25}, probably because of the reduced water solubility of the whole protein as compared to the peptide. It should also be noted that the isotherms of 10 and 20 wt% SP-B_{1-25} in PA monolayers displayed a flattened region between 15 and 22 mN m^{-1}. Longo et al. [17] suggested that the kink at the beginning of the flattened region (point d in Fig. 3(A)) might be the onset of a two-phase coexistence; fluorescence microscopy images (Fig. 4), however, show that this interpretation is incorrect.

Fig. 4 shows fluorescence micrographs of binary mixtures of PA and SP-B_{1-25}. For pure PA at 16°C, a two-phase coexistence between gas and liquid-condensed phase was observed at zero applied pressure. Compressing the system past the lift-off area led to the disappearance of the gas phase, leaving a uniform, gray liquid-condensed phase (Fig. 4(A)). When SP-B_{1-25} was included in the spreading mixture, a three-phase coexistence was observed upon spreading (at zero applied surface pressure), a black gaseous phase, a gray liquid-condensed phase, and a bright "fluid" phase being formed. Upon lift-off, the gas phase disappeared, and a two-phase coexistence remained. Even with a peptide fraction of 5 wt%, the liquid-condensed phase was broken up into dark domains floating in a bright background (Fig. 4(B)). As the percentage of peptide increased, the average size of the dark condensed phase domains decreased while the number density increased (see Fig. 4(C,D)). Similar fluidizing effects were observed in binary mixtures of PA and SP-B_{1-78} (Fig. 5). The peptide apparently disorders or "melts" the condensed phase of PA, as shown by the partitioning of the dye into the new, peptide-rich, bright "fluid" phase. The protein has been shown to be surface-active, possessing an amphipathic α-helical structure in both lipid and aqueous environment, with the hydrophobic residues on one side of the helix and the charged residues on the other [15,16,18,38]. It is plausible therefore that the hydrophobic portion of the peptide is incorporated into the chains, while the positively charged portion is associated with the negatively charged headgroups of PA. The protein also acts to increase the amount of interface between the liquid-condensed and the "fluid" phase, which implies that it may reduce the effective line tension between the two coexisting phases.

Instead of signifying the onset of a two-phase coexistence (that already exists after lift-off), the

Fig. 3. Surface pressure versus area per fatty acid molecule isotherms for PA/SP-B_{1-25} and PA/SP-B_{1-78} mixtures: (A) at 16°C on Milli-Q water subphase (pH 5.5); (B) at 16°C on $NaHCO_3$-buffered saline subphase (pH 6.9, 150 mM NaCl); (C) at 25°C on $NaHCO_3$-buffered saline subphase (pH 6.9, 150 mM NaCl). 0 wt% SP-B_{1-25} (———); 5 wt% SP-B_{1-25} (□); 10 wt% SP-B_{1-25} (▽); 20 wt% SP-B_{1-25} (○); 20 wt% SP-B_{1-78} (×). The marked points signify (a) the beginning of the liquid-condensed phase, (b) the transition to the solid-condensed phase, (c) film collapse, (d) onset of the flattened portion of the isotherm, (e) the beginning of the liquid-expanded/liquid-condensed coexistence. The peptide increases the collapse pressure of the monolayer, leading to lower surface tensions on compression. All mixtures contain 1 mol% (with respect to the PA concentration) of NBD-HDA, which does not appear to alter the isotherms significantly.

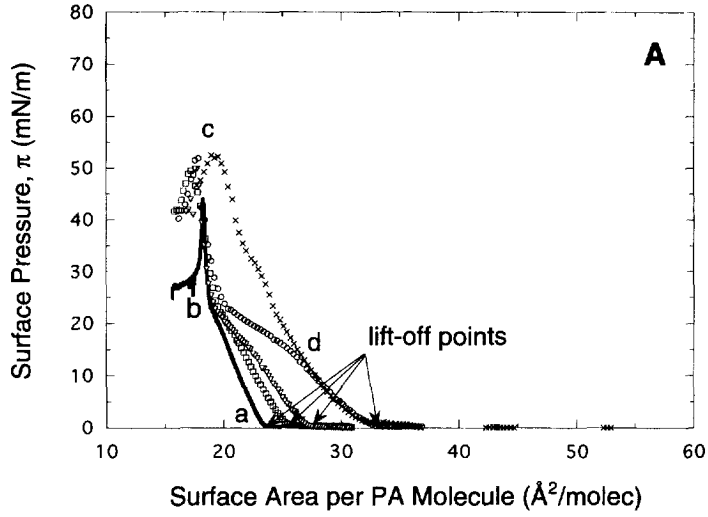
A
Surface Pressure, π (mN/m)
Surface Area per PA Molecule (Å²/molec)
c
b
d
a
lift-off points

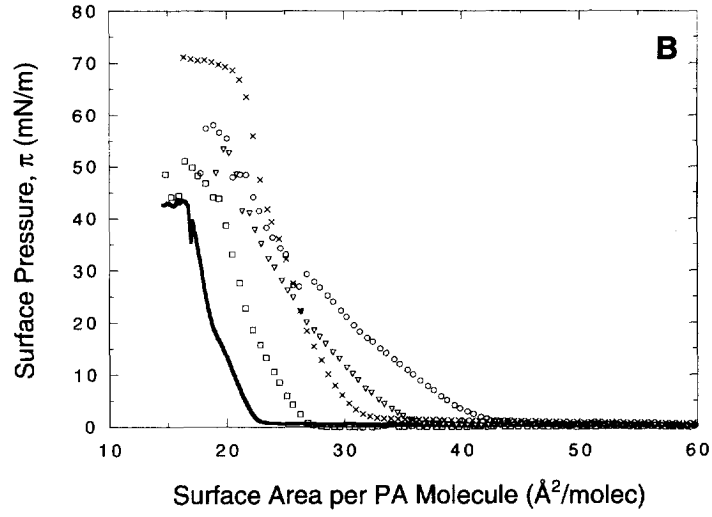
B
Surface Pressure, π (mN/m)
Surface Area per PA Molecule (Å²/molec)

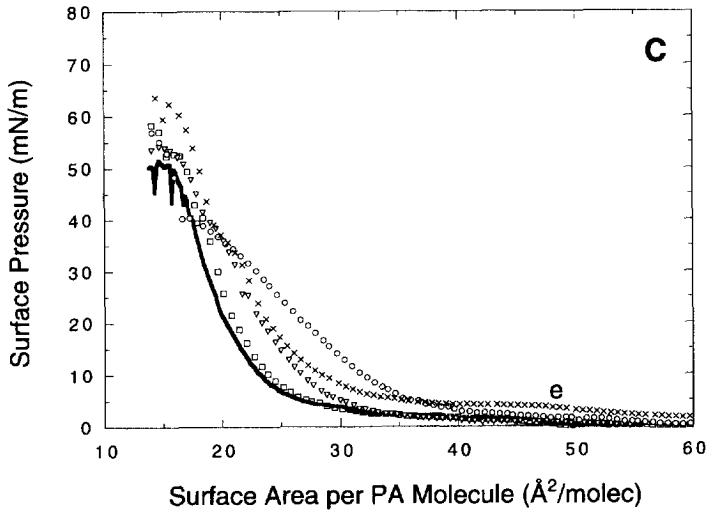
C
Surface Pressure (mN/m)
Surface Area per PA Molecule (Å²/molec)
e

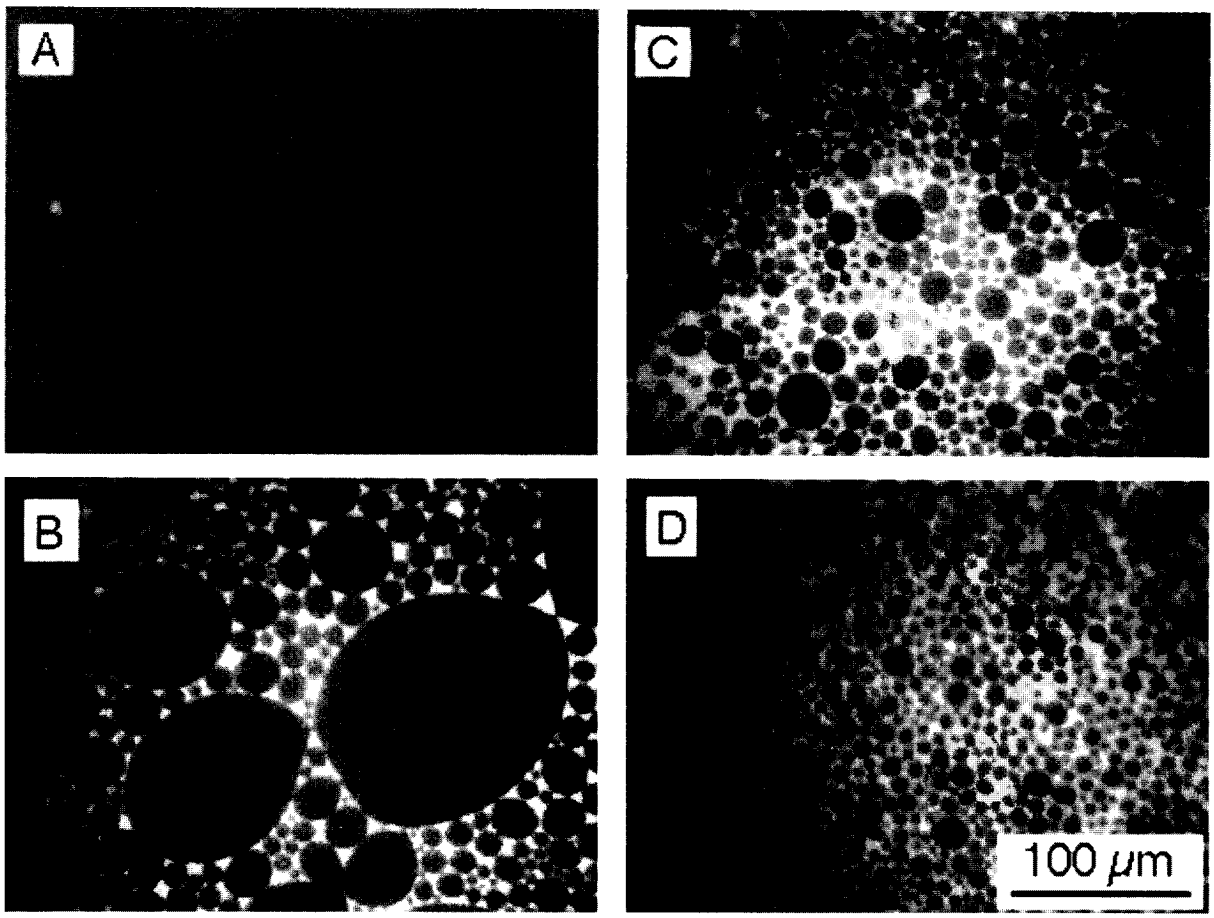

Fig. 4. Fluorescence micrographs of PA/SP-B_{1-25} mixtures at 16°C on Milli-Q water subphase (pH 5.5): (A) 0 wt% peptide; (B) 5 wt% peptide; (C) 10 wt% peptide; (D) 20 wt% peptide. All mixtures contain 1 mol% (with respect to the PA concentration) of NBD-HDA fluorescent dye. All images were taken at the lift-off point. The peptide inhibits the formation of the condensed phase, leading to the formation of a disordered, bright fluid phase that separates the remaining condensed phase domains. The line tension between the two phases is small as indicated by a steady decrease in the condensed phase domain size with increasing peptide concentration. The image contrast results from the exclusion of the dye from the more ordered, condensed phases (dark), and its incorporation in the more disordered, expanded phases (bright).

flattened portion of the isotherm in monolayers with high peptide fraction may mark the onset of the removal of excess peptide from the monolayer. Fluorescence micrographs show that the kink occurs when condensed phase domains start to close-pack. Should the peptide have a pressure-dependent solubility that increases as a function of surface pressure, the kink in the isotherm would signify the onset of an abrupt increase in peptide solubility, rendering the film more compressible and flattening out the isotherm. This hypothesis is corroborated by isotherms obtained for pure SP-B_{1-25} at the air–water interface that show flattened portions starting at surface pressures similar to those found in lipid–protein monolayers (point d in Fig. 3(A)).

3.2. *Buffered saline subphase at 16°C*

To study the effects of charge and ionic strength and to better mimic physiological conditions, a $NaHCO_3$-buffered saline (pH 6.9, 0.15 M NaCl)

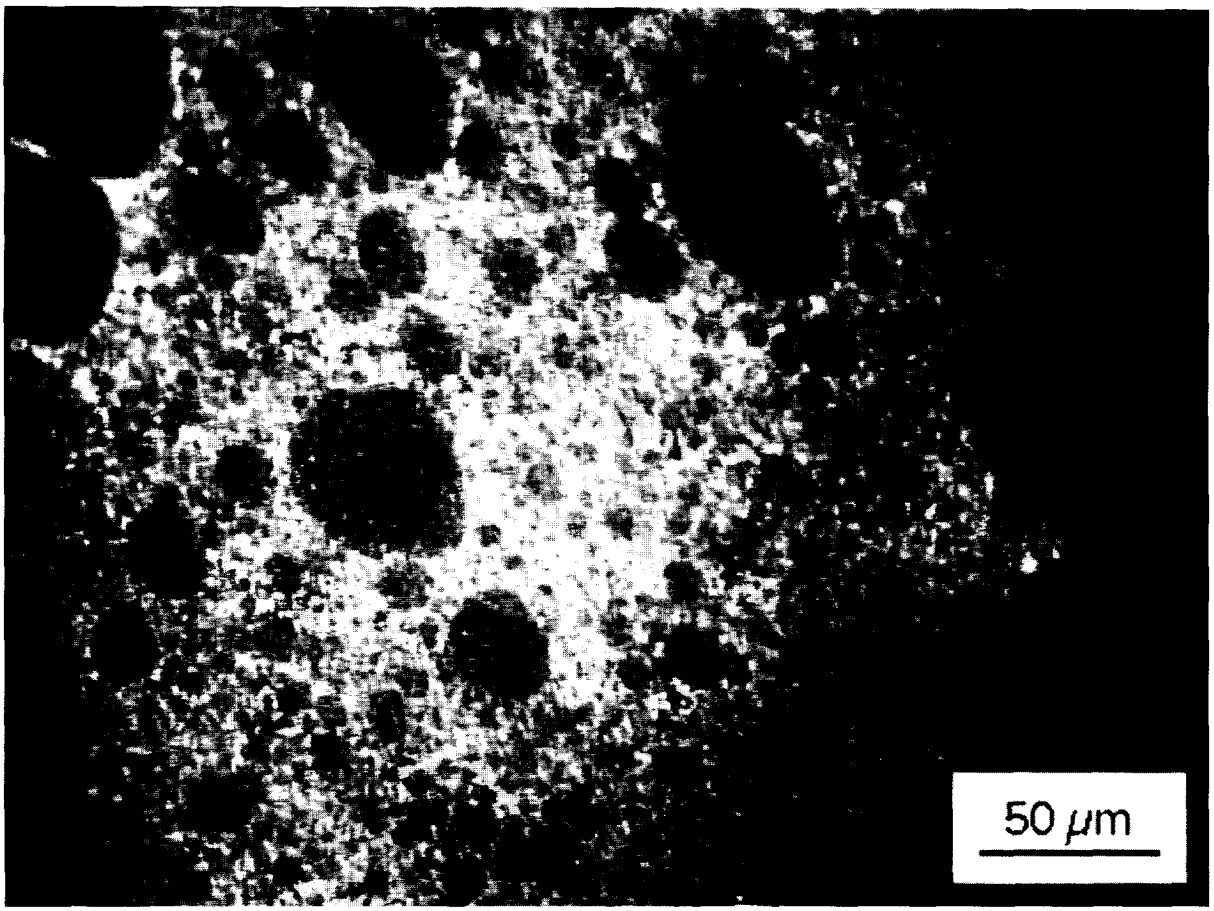

Fig. 5. Fluorescence micrograph of PA/SP-B_{1-78} mixtures with 20 wt% peptide at 16°C on Milli-Q water subphase (pH 5.5), and 1 mol% (with respect to the PA concentration) of NBD-HDA fluorescent dye. Image taken at the lift-off point.

subphase was used. The temperature was kept at 16°C for direct comparisons with the first set of experiments. A similar rise in collapse pressures and lift-off areas was observed when the fraction of peptide was increased. However, the collapse pressures for monolayers on a saline subphase were higher (Fig. 3(B)) than those on pure water (Fig. 3(A)); in the case of SP-B_{1-78}, a collapse pressure close to 72 mN m^{-1} was achieved. Furthermore, isotherms of 10 and 20 wt% SP-B_{1-25} no longer displayed a flattened region. The increase in collapse pressure could be due to the increased surface dissociation at higher pH, which in turn increased the activation energy for the film to collapse [39,40], whereas the disappearance of the flattened region could be attributed to the decreased solubility of the peptide in saline solutions [41]. For the most part, the surface morphology was similar to that on pure water: the condensed phase of PA was broken up by the presence of a bright phase when peptide was added, and the condensed phase domain size decreased as the fraction of peptide was increased. However, one significant morphological difference was noted.

When a mixture of PA with a high percentage of peptide (over 20 wt% SP-B_{1-25} or SP-B_{1-78}) was spread on the saline subphase, alternating linear domains of high and low lipid concentration, or "stripe" patterns [31], were observed at zero

applied pressure (Fig. 6(A,B)). Similar stripe patterns are found in pure SP-B_{1-25} films. Fig. 6(C) shows stripes in a fluorescein-tagged SP-B_{1-25} monolayer on a water subphase at zero applied surface pressure and 23°C. The ratio of dark to bright phases increased with increasing surface area, and eventually gave rise to an extended foam-like appearance (Fig. 6(D)). In mixed lipid and protein monolayers, we have also observed circular domains undergoing shape transitions to form labyrinthine patterns upon compression at zero surface pressure (Fig. 7). Several researchers have observed stripe phases together with shape transitions in monolayers at the air–water interface [42–45]. The transition between circular and stripe domains can be understood in terms of a competition between the line tension at the domain boundary and the electrostatic repulsion within the domain. In the limit of large line tensions, circular domains are preferred because this minimizes the length of the domain boundary. When the line tension decreases relative to the repulsive interactions within the domains, elongated shapes or stripe phases form. Because stripes were not observed in mixed monolayers with low protein content even on a saline subphase, and were pre-

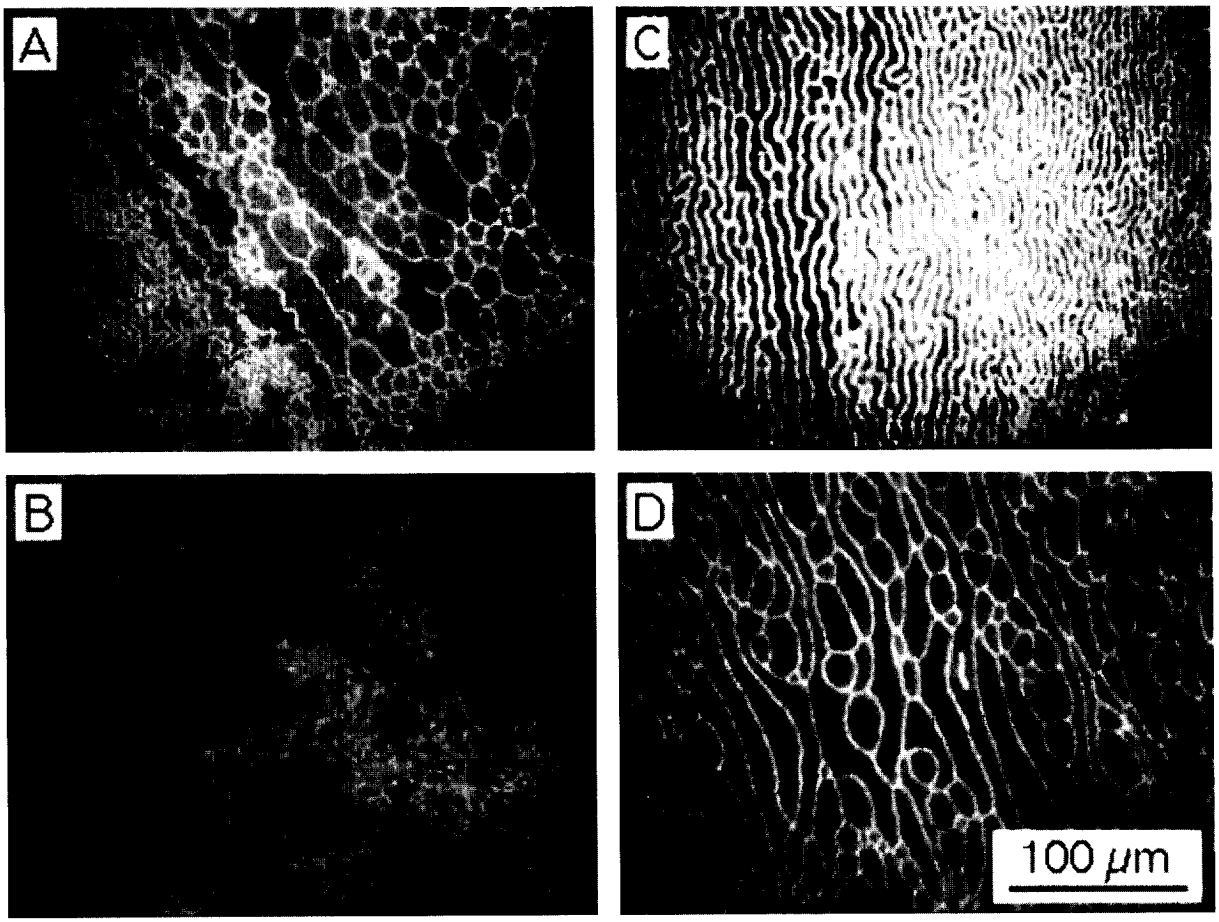

Fig. 6. Fluorescence micrographs of stripe patterns observed in a monolayer from (A) a PA/SP-B_{1-25} mixture with 20 wt% peptide on $NaHCO_3$-buffered saline subphase (pH 6.9, 150 mM NaCl) at 16°C and zero surface pressure; (B) a PA/SP-B_{1-78} mixture with 20 wt% peptide on $NaHCO_3$-buffered saline subphase (pH 6.9, 150 mM NaCl) at 16°C and zero surface pressure; (C) a pure fluorescein-labelled SP-B_{1-25} monolayer on Milli-Q water subphase (pH 5.5) at 23°C and zero surface pressure; (D) the same film as in (C) but at a larger surface area per fatty acid molecule.

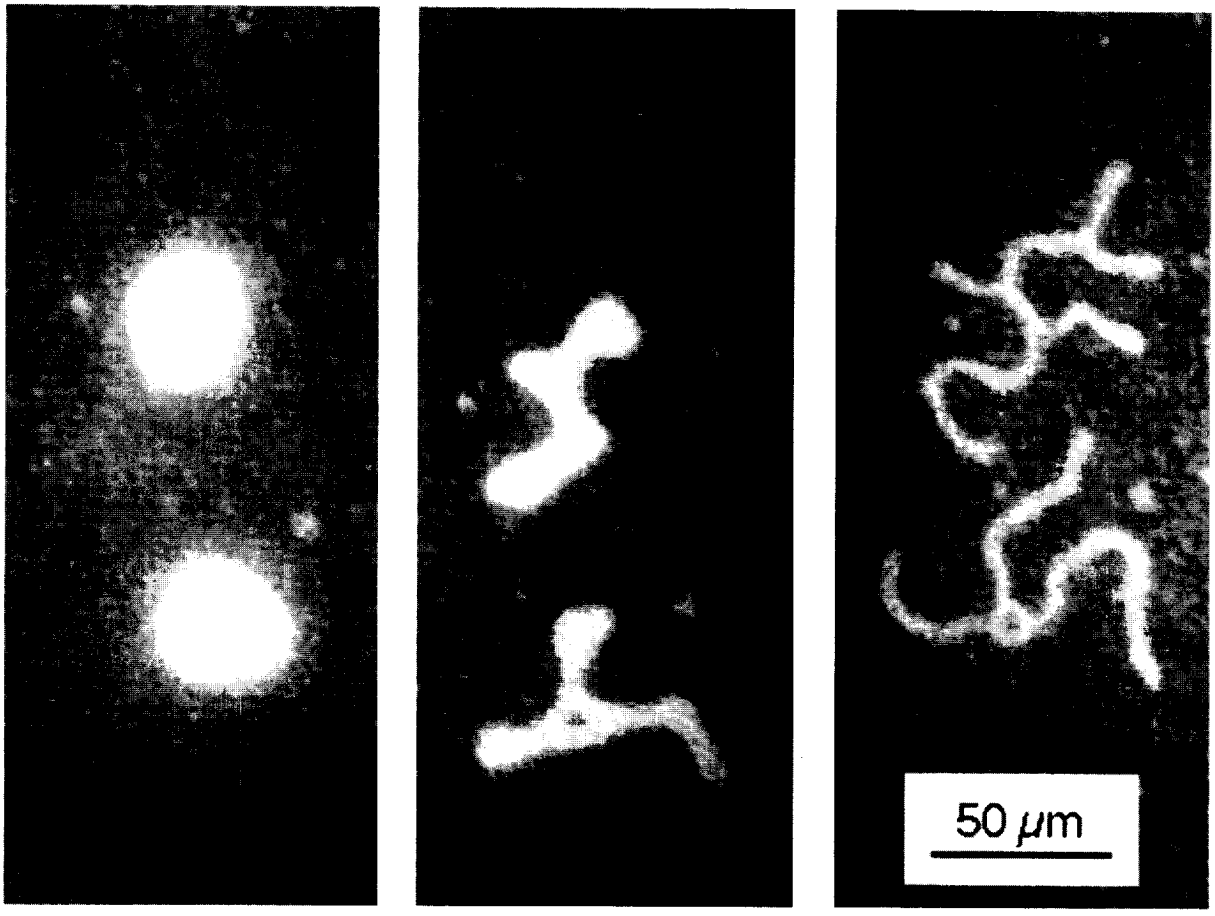

Fig. 7. A sequence in which two bright circular domains in a PA/SP-B_{1-25} mixture with 20 wt% peptide on $NaHCO_3$-buffered saline subphase transform into two labyrinthine patterns with decreasing surface area at zero surface pressure. The transformation shows that the ratio of electrostatic repulsion within the domain to the line tension at the domain boundary changes upon compression, perhaps due to a conformational change in the protein.

sent in pure protein monolayers on a pure water subphase, the stripe patterns are inherent to the protein. These results, combined with theoretical and experimental observations that stripe formation typically occurs in mixed monolayers [32,46], suggest that the protein undergoes a surface pressure-induced conformational, orientational and/or aggregational change, which leads to a change in the relative contribution between the line tension and the electrostatic interactions. Both surface pressure and lipid environment induced protein conformational changes have been shown to occur in similar systems [47].

3.3. *Buffered saline subphase at 25°C*

In order to examine films that have phase behavior similar to those under physiological conditions, we carried out a set of experiments above the triple point temperature of PA. At 25°C on a buffered saline subphase, the isotherm of the fatty acid showed a gas/liquid-expanded coexistence region at large molecular areas. The system entered a liquid-expanded region after lift-off, followed by a plateau where liquid-expanded and liquid-condensed phases coexisted. Further increases in pressure led to the liquid-condensed phase, then the

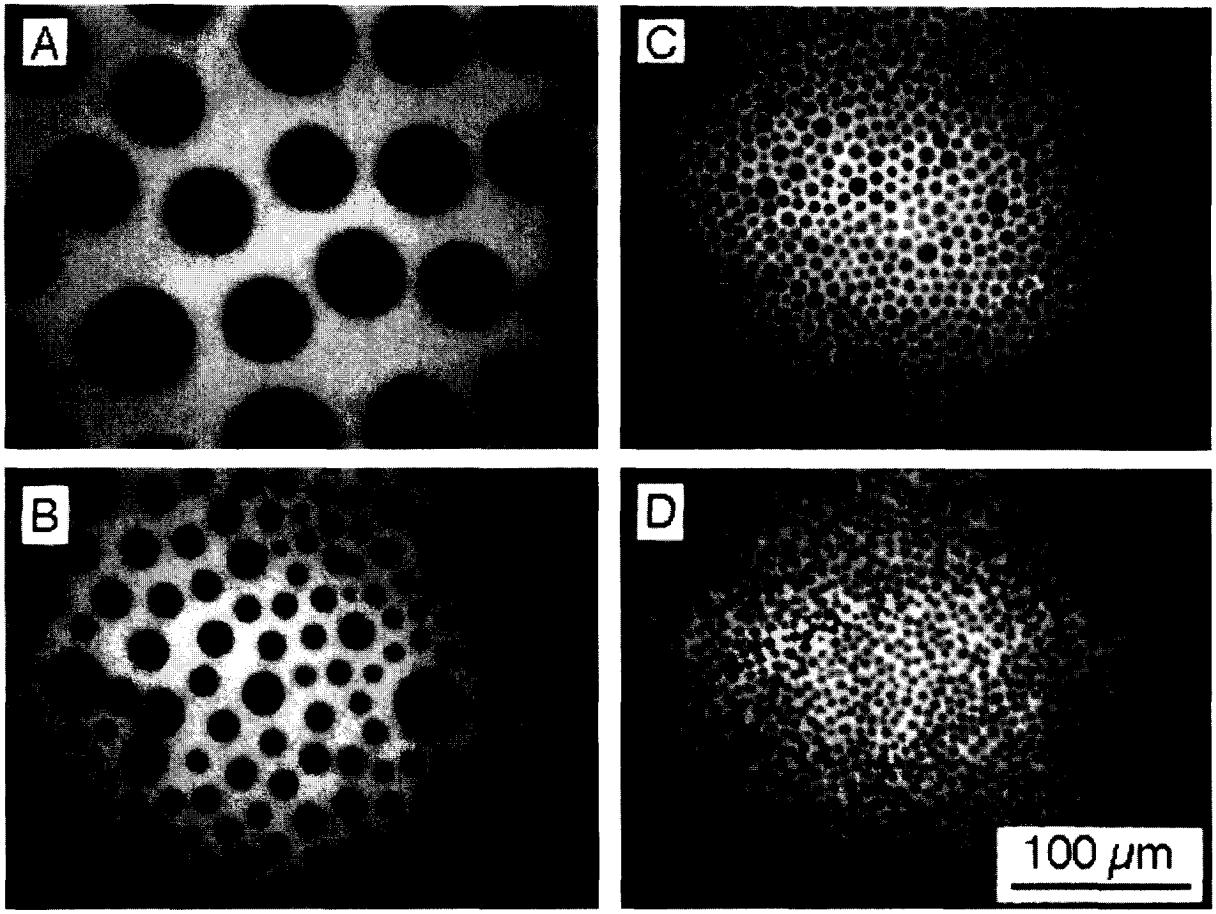

Fig. 8. Fluorescence micrographs of PA/SP-B_{1-25} mixtures at 25°C on $NaHCO_3$-buffered saline subphase (pH 6.9, 0.15 mM NaCl): (A) 0 wt% peptide; (B) 5 wt% peptide; (C) 10 wt% peptide; (D) 20 wt% peptide. All mixtures contain 1 mol% (with respect to the PA concentration) of NBD-HDA. Image taken at an area per PA molecule of 35 $Å^2$.

solid-condensed phase, and eventually monolayer collapse at about 52 mN m^{-1}. Addition of either the full length protein or the shorter model peptide resulted in a similar rise in collapse pressures and lift-off areas as in low temperature films (see Fig. 3(C)).

Below the triple point, the dark liquid-condensed phase (Fig. 4) was present upon spreading; hence, the initial distribution of the domains was influenced by the spreading conditions. Above the triple point, however, the liquid-condensed or dark phase nucleated from the liquid-expanded phase at the beginning of the liquid-expanded/liquid-condensed plateau (Fig. 3(C), point e). As a result, the effect of the addition of the peptide on the formation and size of domains is more dramatic. In the absence of the peptide, dark domains nucleated with low number density from the bright phase, and grew into large domains (Fig. 8(A)). Fig. 8(B,C,D) shows how the number density of domains successively increased while the average size successively decreased with increasing percentage of SP-B_{1-25} present. The progression observed is reminiscent of that found below the triple point (Fig. 4). When full length SP-B_{1-78} is added, a similar type of small-size, high-density nucleation of condensed phase domains was observed (Fig. 9).

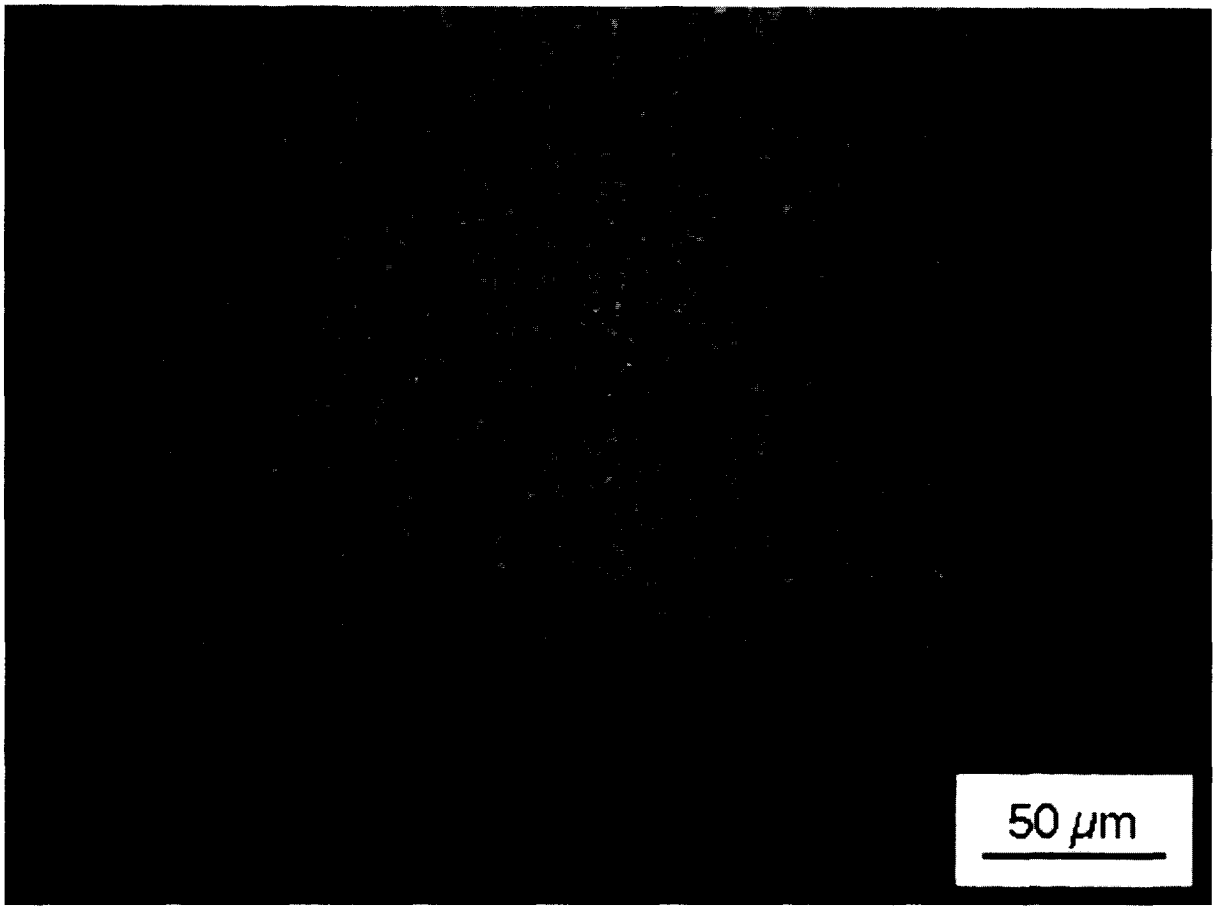

Fig. 9. Fluorescence micrograph of PA/SP-B_{1-78} mixtures with 20 wt% peptide at 25°C on $NaHCO_3$-buffered saline subphase (pH 6.9, 0.15 mM NaCl), and 1 mol% (with respect to the PA concentration) of NBD-HDA fluorescent dye. Image taken at an area per PA molecule of 35 Å^2.

3.4. Collapse mechanism

In all the above experiments, we found that collapse pressures were increased with the incorporation of either the full length or the shorter model peptide into the fatty acid film. To understand such increases in collapse pressure, we compressed the film past collapse, and, in the process, observed differences in the nucleation, growth and morphology of monolayer collapse when protein was added to PA monolayers.

Fig. 10(A,B) shows the collapse structures present at 16°C on a pure water subphase with and without SP-B_{1-25}, respectively. Without the peptide, large, dendritic "crystals" that grew with time appeared at collapse (Fig. 10(B)). With the peptide, no large crystals were observed; instead, very small, bright collapse structures nucleated simultaneously over the entire monolayer at a significantly higher surface pressure, and remained small, even upon further compression (Fig. 10(A)). Similar collapse structures were also observed for PA/SP-B_{1-78} films. The collapse structures of a PA film with 20 wt% SP-B_{1-25}, and a pure PA film at 27°C, again on a pure water subphase, are shown respectively in Fig. 10(C,D). Although there were differences in the morphology of the collapse structures due to temperature [48], the general features of collapse were the same: without the peptide, large dendritic structures nucleated at the collapse

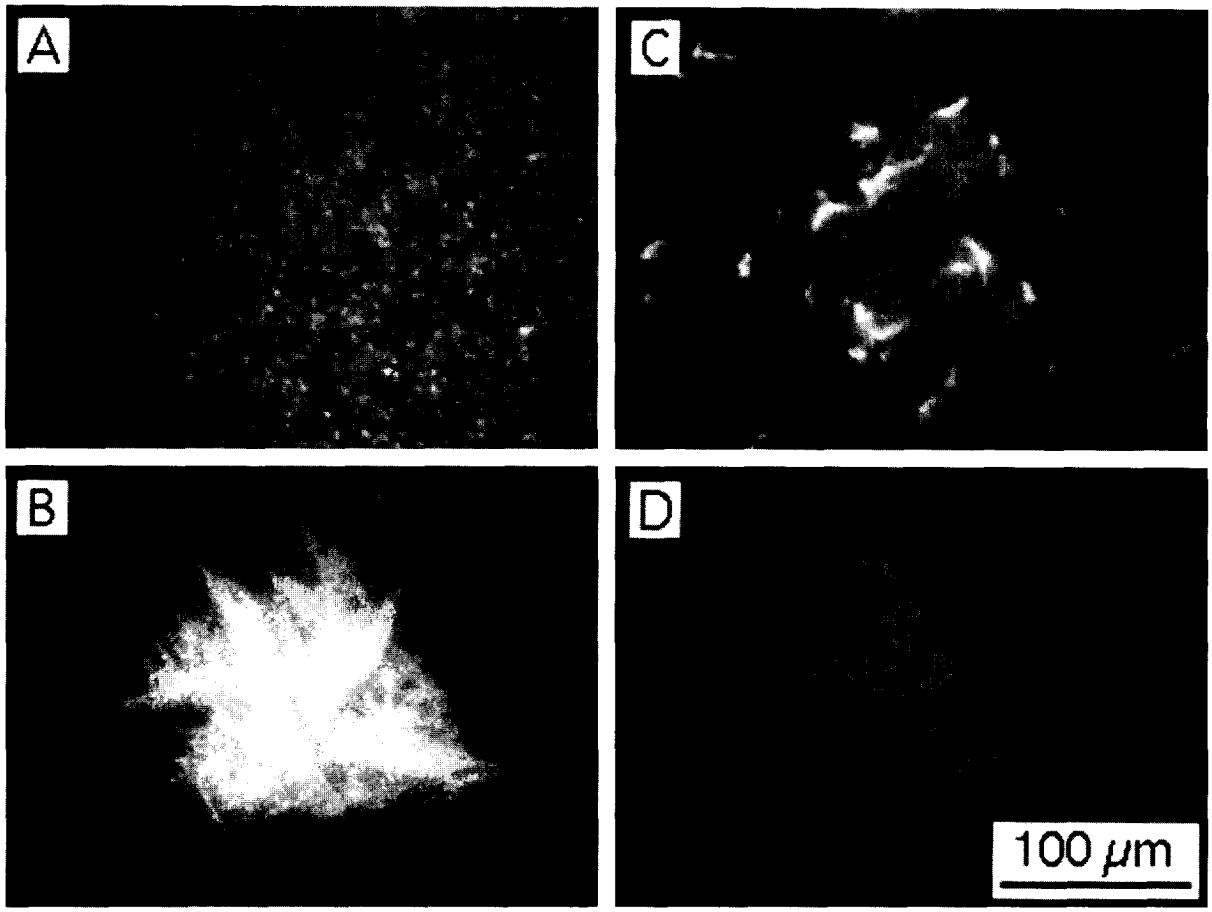

Fig. 10. Collapse structures of PA films with and without SP-B_{1-25} on Milli-Q water subphase (pH 5.5) at two different temperatures. (A) Small bright collapse structures nucleate from condensed phase domains on collapse of a monolayer of a PA/SP-B_{1-25} mixture with 20 wt% peptide at 16°C. The small spots disappear quickly on respreading. (B) Large dendritic crystals occur on collapse of a pure PA monolayer at 16°C. These crystals grow with time and are slow to respread on expansion. (C) A network of bright "fluid" phases remains at collapse pressure for a PA/SP-B_{1-25} mixture with 20 wt% peptide at 27°C. Small, bright collapse structures nucleate uniformly across the monolayer and respreading is easy. (D) Large dendritic crystals occur on collapse of a pure PA monolayer at 27°C. Similar to their counterparts at a lower temperature, these crystals grow with time and are slow to respread. Differences observed in collapse features between (A) and (C), and (B) and (D) suggest that temperature affects collapse structures.

pressure and quickly grew (Fig. 10(D)); with the peptide present, much smaller and more numerous bright collapse structures appeared at a higher collapse pressure (Fig. 10(C)). Fig. 10(C) also shows that the dark condensed phase domains are subdivided by a skeletal network of light-gray fluid phase. The network thinned as the surface pressure increased, but persisted even after the film collapsed, suggesting that the peptide–fatty acid complex was retained in the film. Similar networks were observed for PA/SP-B_{1-25} and PA/SP-B_{1-78} monolayers with 20 wt% peptide at temperatures both above (Fig. 11(A,B)) and below (data not shown) the triple point on buffered saline subphases up to and after collapse.

The existence of the mesh provides an explanation for the difference in collapse pressures and morphology. From our images it is clear that monolayer collapse occurs by a process of nucleation and growth. By breaking up the condensed phase into small domains, the fluid network lowers the probability that a collapse "nucleus" can be

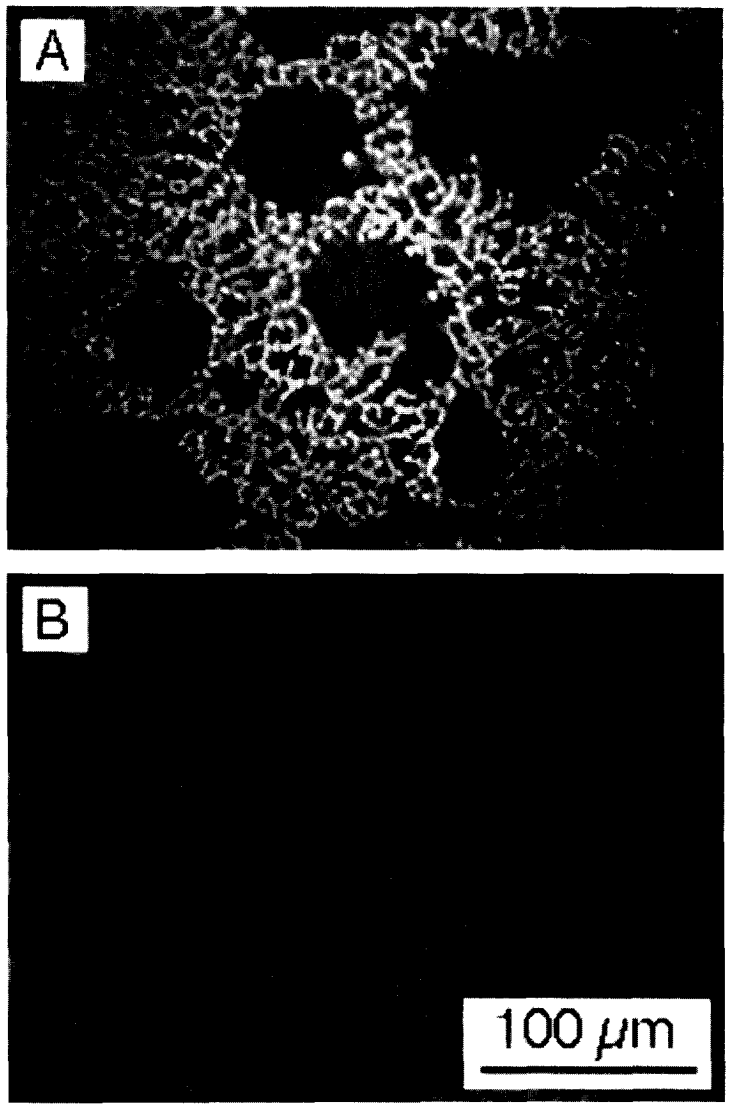

Fig. 11. A network of bright "fluid" phases observed near the collapse pressure for (A) a PA/SP-B_{1-25} mixture with 20 wt% peptide, and (B) a PA/SP-B_{1-78} mixture with 20 wt% peptide at 16°C on $NaHCO_3$-buffered saline subphase (pH 6.9, 150 mM NaCl), separating regions of dark condensed phase.

found in a given domain [49,50]. As a result, each domain must nucleate collapse independently, resulting in more uniform, homogeneous nucleation at higher surface pressures. This phenomenon is the two-dimensional analog of the classic experiments of Turnbull, who showed that many simple metallic liquids could be undercooled far below their thermodynamic freezing points by subdividing the liquid into micrometer-sized droplets [51]. Subdividing the droplets reduced the likelihood of a heterogeneous nucleus in a given droplet, leading to homogeneous nucleation at large undercooling. Similar effects have been observed for supercooling water in emulsion droplets, in polymer gels, or in porous media [52,53]. Even after this homogeneous nucleation, the growth of the collapse structures is limited by the finite size of the condensed domains. As a result,

the collapse structures are small in size in the case of homogeneous nucleation compared to those found in heterogeneous nucleation. Hence respreading of these small collapse structures on expansion occurs much more readily. In the absence of the peptide (Fig. 10(B,D)), the large, dendritic "crystals" that formed at collapse grew with time and were much more difficult to respread upon expansion. It is therefore clear that one function of lung surfactant specific protein SP-B is to form a network of fluid phase that breaks up the condensed phase domains, thereby altering the nucleation and growth of monolayer collapse, leading to lower ultimate surface tensions on compression and easier respreading on expansion.

4. Conclusions

Our results show that the shorter model peptide SP-B_{1-25} mimics quite closely the behavior of the full length protein SP-B_{1-78}, causing similar alterations to the isotherm, and similar changes in the surface morphology and collapse mechanism of fatty acid monolayers. Isotherm measurements show that the lift-off area increases with increasing amount of protein in the fatty acid monolayer, signifying that the protein is indeed incorporated into the monolayer. The presence of the protein also leads to higher collapse pressures, which in some cases can reach a value close to 72 mN m^{-1} (equivalent to attaining zero surface tension). These changes in the isotherm remove the driving force for squeeze-out of the PA from monolayers of DPPC, a major component of lung surfactant. We believe that the interaction between PA and either the full length protein or the shorter model peptide is electrostatic in nature, with the hydrophobic portions of the protein associating with the tails of the fatty acid, while the positively charged regions complex with the negatively charged headgroups. The effect both SP-B_{1-78} and SP-B_{1-25} have on the isotherms of fatty acid monolayers is almost identical to that of simple polycations [20]. Effective replacement surfactants could possibly include simple polymers or amino acid sequences instead of native SP-B.

Epifluorescence microscopy images show that both the positively charged full length SP-B_{1-78} and its N-terminal segment SP-B_{1-25} insert into PA monolayers and inhibit the formation of the condensed phases at all surface pressures. The presence of the protein leads to the formation of a protein-rich fluid phase in coexistence with the condensed PA phase. The fluid phase persists up to collapse, forming a network separating the condensed phase into domains, with domain size decreasing as the protein content increases. The existence of the network indicates that the protein is retained in the monolayer even at high compression. In pure PA monolayers, collapse occurs by the nucleation and growth of large, three-dimensional dendritic "crystals" from the solid-condensed phase. With the presence of SP-B_{1-78} or SP-B_{1-25}, a new type of nucleation occurs at higher surface pressures (lower surface tensions). These new collapse structures occur much more uniformly across the monolayer, are much smaller in size, and hence are much easier to respread on lowering the surface pressure. These effects suggest a dramatic change in collapse nucleation; heterogeneous, lower surface pressure nucleation occurs without protein and homogeneous, higher surface pressure nucleation occurs with protein. After collapse, the growth of the collapse structures in the presence of protein is limited by the finite size of the solid-condensed domains, and they are hence easier to respread on expansion. Stripe patterns, indicative of low line tensions [42–44], are found both in fatty acid films with a high percentage of protein on a saline subphase and in films formed by fluorescein-tagged SP-B_{1-25} on pure water subphase, and help to explain the stability of the fluid phase network. This lowered line tension may be associated with a pressure induced conformational, orientational and/or aggregational change of the protein.

Our observations here help explain our earlier work [15,18] and that of Cochrane and Revak [19], and Venkitaraman et al. [36], who observed greater enhancements of surface activity for monolayers with amino acid sequences that contained cationic residues than for those that were primarily hydrophobic or anionic. The fact that the phase behavior and morphology of charged fatty acids can be dramatically altered by interactions with

charged synthetic peptides or polymers points to the possibility that these electrostatic interactions might be the origin of lung surfactant inhibition by charged soluble proteins such as albumin or fibrinogen that are believed to be responsible for the onset of adult RDS. The detailed picture of the role of SP-B in the monolayer presented in this paper should make it possible to develop synthetic peptides or even simple polymers for new replacement surfactants, and shows that many of the essential features of the whole protein are captured by the N-terminal segment.

References

[1] F. Possmayer, S. Yu, J. Weber, P. Harding, Can. J. Biochem. Cell Biol. 62 (1984) 1121.

[2] K. Shiffer, S. Hawgood, N. Duzgunes, J. Goerke, Biochemistry 27 (1988) 2689.

[3] R.J. King, in: E. Robertson, L.M.G. Van Golde, J.J. Batenburg (Eds.), Pulmonary Surfactant, Elsevier, Amsterdam, 1984, p. 1.

[4] D.L. Shapiro, R.H. Notter (Eds.), Surfactant Replacement Therapy, Liss, New York, 1989.

[5] M.E. Avery, J. Mead, Am. J. Dis. Child. 97 (1959) 917.

[6] J.A. Clements, Arch. Environ. Health 2 (1961) 280.

[7] A. Jobe, M. Ikegami, Am. Rev. Respir. Dis. 136 (1987) 1256.

[8] K. Keough, C. Parsons, P. Phang, M. Tweeddale, Can. J. Physiol. Pharmacol. 66 (1988) 1166.

[9] W. Seeger, A. Gunther, C. Thede, Am. J. Physiol. 261 (1992) L286.

[10] R. Soll, Resident Staff Physician 38 (1992) 19.

[11] R. Schwartz, M. Anastasia, M. Luby, J. Scanlon, R. Kellogg, New Engl. J. Med. 330 (1994) 1476.

[12] J. Whitsett, W. Hull, B. Ohning, G. Ross, T. Weaver, Pediatr. Res. 20 (1986) 744.

[13] S.-H. Yu, F. Possmayer, Biochem. J. 236 (1986) 85.

[14] S. Hagwood, B.J. Benson, J. Schilling, D. Damm, J.A. Clements, R.T. White, Proc. Natl. Acad. Sci. USA 84 (1987) 66.

[15] A. Waring, W. Taeusch, R. Bruni, J. Amirkhanian, B. Fan, R. Stevens, J. Young, Peptide Res. 2 (1989) 308.

[16] A. Waring, R. Stevens, J. Young, R. Bruni, W. Taeusch, Biophys. J. 59 (1991) 507a.

[17] M.L. Longo, A.M. Bisagno, J.A. Zasadzinski, R. Bruni, A.J. Waring, Science 261 (1993) 453.

[18] R. Bruni, H. Taeusch, A. Waring, Proc. Natl. Acad. Sci. USA 88 (1991) 7451.

[19] C. Cochrane, S. Revak, Science 254 (1991) 566.

[20] L.F. Chi, R.R. Johnson, H. Ringsdorf, Langmuir 7 (1991) 2323.

[21] T. Curstedt, H. Jornvall, B. Robertson, T. Bergman, P. Berggren, Eur. J. Biochem. 168 (1987) 255.

[22] S.-H. Yu, F. Possmayer, Biochim. Biophys. Acta 961 (1988) 337.

[23] The surface pressure π is the difference between the bare water surface tension (72 mN m^{-1}) and the measured surface tension. The collapse pressure of a monolayer is the highest surface pressure attainable before the film collapses, or ejects material into a bulk phase.

[24] M. Longo, A. Waring, J. Zasadzinski, Biophys. J. 63 (1992) 760.

[25] A. Cockshutt, D. Absolom, F. Possmayer, Biochim. Biophys. Acta 1085 (1991) 248.

[26] PA is one of three additives to exogenous surfactant in Survanta (Ross Laboratories) and Surfactant TA (Tokyo Tanabe) used to treat premature infants suffering neonatal RDS. PA is added to lipid extract surfactant (LES), an acetone precipitate of animal surfactant with fatty acids and triacylglycerols removed, to enhance the surface activity and partially counteracts inhibition by blood proteins [25,27–29]. However, PA does not prevent inhibition by blood proteins of synthetic mixtures which are lung surfactant protein-free [30]. Tanaka et al. have developed a primarily synthetic surfactant that contains DPPC, unsaturated phosphatidylglycerol (PG), PA, and an animal lung protein extract containing mainly SP-B [54]. PA is also added to KL_4-surfactant, a synthetic surfactant incorporating a model lysine–leucine peptide instead of SP-B [19].

[27] J. Chung, R. Hannemann, E. Franses, Langmuir 6 (1990) 1647.

[28] N. Mathialagan, F. Possmayer, Biochim. Biophys. Acta 1045 (1990) 121.

[29] S.-H. Yu, F. Possmayer, Biochim. Biophys. Acta 1126 (1992) 26.

[30] B. Holm, A. Venkitaraman, G. Enhorning, R. Notter, Chem. Phys. Lipids 52 (1990) 243.

[31] M. Seul, D. Andelman, Science 267 (1995) 476.

[32] H.M. McConnell, V.T. Moy, J. Phys. Chem. 92 (1988) 4520.

[33] C.G. Fields, D.H. Lloyd, R.L. MacDonald, K.M. Ottenson, R.L. Noble, Peptide Res. 4 (1991) 95.

[34] The triple point denotes the location in the phase diagram where the two-dimensional equivalents of the solid (liquid-condensed), liquid (liquid-expanded), and gaseous phase coexist at equilibrium. The triple point temperature PA was found to be 24.8°C on Milli-Q water subphase; the triple point temperature on a saline buffered subphase is lower. Below the triple point, the gaseous phase transforms into the liquid-condensed phase without going through the liquid-expanded phase. Above the triple point, the liquid-condensed and liquid-expanded phases coexist.

[35] M.M. Lipp, K.Y.C. Lee, J.A. Zasadzinski, A.J. Waring, Rev. Sci. Instru. 68 (1997) 2574.

[36] A. Venkitaraman, S. Hall, R. Notter, Chem. Phys. Lipids 53 (1990) 157.

[37] C.C. Cochrane, S.D. Revak, T.A. Merritt, G.P. Heldt, M. Hallman, M.D. Cunningham, D. Easa, A. Pramanik, D.K.

Edwards, M.S. Alberts, Am. J. Respir. Crit. Care Med. 153 (1996) 404.
[38] A. Takahashi, A.J. Waring, J. Amirkhanian, B. Fan, H.W. Taeusch, Biochim. Biophys. Acta 1044 (1990) 43.
[39] S. Xu, K. Miyano, B. Abraham, J. Colloid Interface Sci. 89 (1982) 581.
[40] R. Smith, J. Berg, J. Colloid Interface Sci. 74 (1980) 273.
[41] We have performed experiments with pure SP-B_{1-25} on both a pure water and a saline subphase, and found that the solubility of the protein is lower on saline than on water subphase.
[42] H.M. McConnell, Nature 310 (1984) 47.
[43] M. Seul, M. Sammon, Phys. Rev. Lett. 64 (1990) 1903.
[44] M. Seul, V.S. Chen, Phys. Rev. Lett. 70 (1993) 1658.
[45] K.Y.C. Lee, H.M. McConnell, J. Phys. Chem. 97 (1993) 9532.
[46] J. Stine, D.T. Stratmann, Langmuir 8 (1992) 2509.
[47] M. Briggs, D. Cornell, R. Dluhy, L. Gierasch, Science 233 (1986) 4306.
[48] S. Siegel, D. Hönig, D. Volhardt, D. Möbius, J. Phys. Chem. 96 (1992) 8157.
[49] A.W. Adamson, Physical Chemistry of Surfaces, 5th ed., Wiley, New York, 1990.
[50] R.J. Hunter, Foundations of Colloid Science, Vol. 1, Ch. 7, University Press, Belfast, 1992.
[51] D. Turnbull, J. Chem. Phys. 20 (1952) 411.
[52] P. Bruggeller, E. Mayer, Nature 288 (1980) 569.
[53] T. Tanaka, S. Ishiwata, C. Ishimoto, Phys. Rev. Lett. 38 (1977) 771.
[54] Y. Tanaka, T. Tsunetomo, A. Toshimitsu, K. Masuda, K. Akira, T. Fujiwara, J. Lipid Res. 000 (1986) 475.